Electronic Supplementary Material (ESI) for Dalton Transactions.


# Supporting Information

## Temperature dependent NIR emitting lanthanide-PMO/silica hybrid materials

Anna M. Kaczmarek,‡*[,a] Dolores Esquivel,‡[b] Judith Ouwehand,[c] Pascal Van Der Voort,[c] Francisco J. Romero-Salguero,[b] Rik Van Deun*[,a]

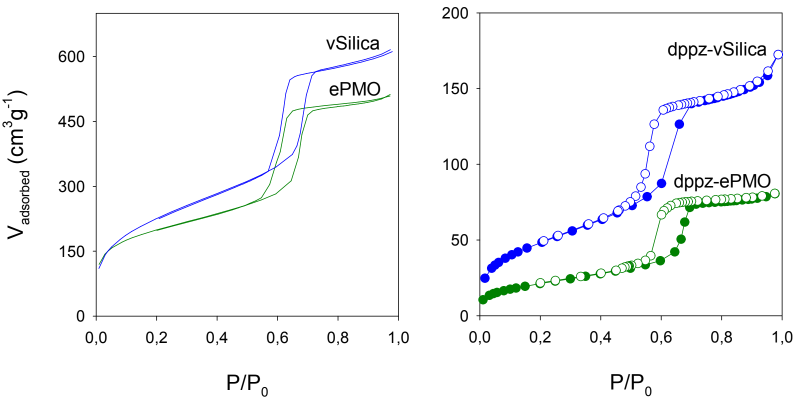


Fig. S1 $N_2$ adsorption-desorption isotherms of the parent materials (left) and dipyridyl-pyridazine functionalized materials (right).

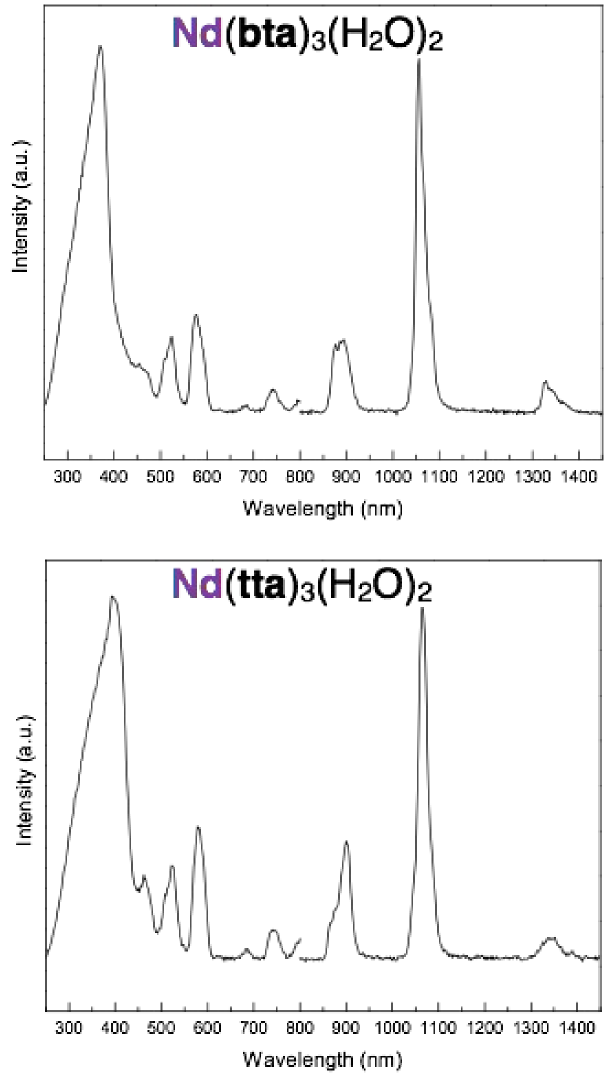


Fig. S2 Combined excitation-emission spectra of $Nd^{3+}$ β-diketonate complexes (the spectra were recorded by exciting into the maximum of the broad excitation band and observing at the maximum of the strongest emission peak).

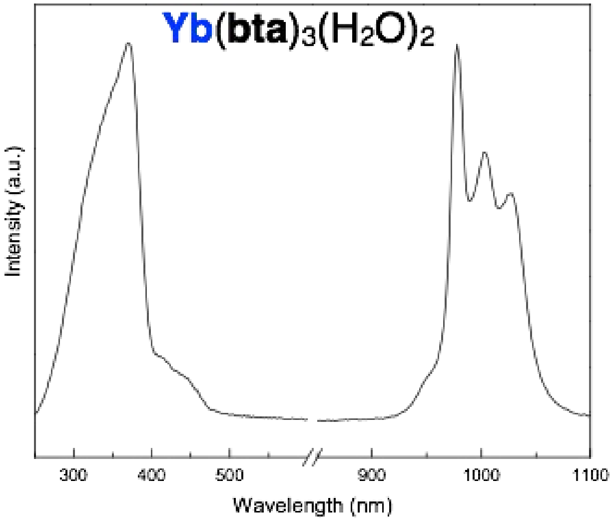


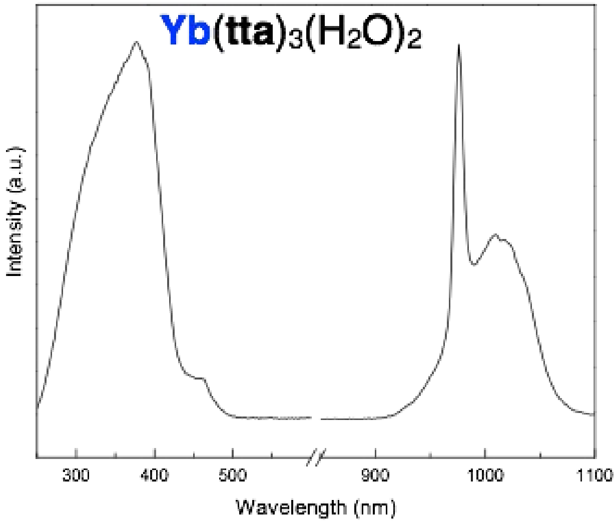


Fig. S3 Combined excitation-emission spectra of $Yb^{3+}$ β-diketonate complexes (the spectra were recorded by exciting into the maximum of the broad excitation band and observing at the maximum of the strongest emission peak).

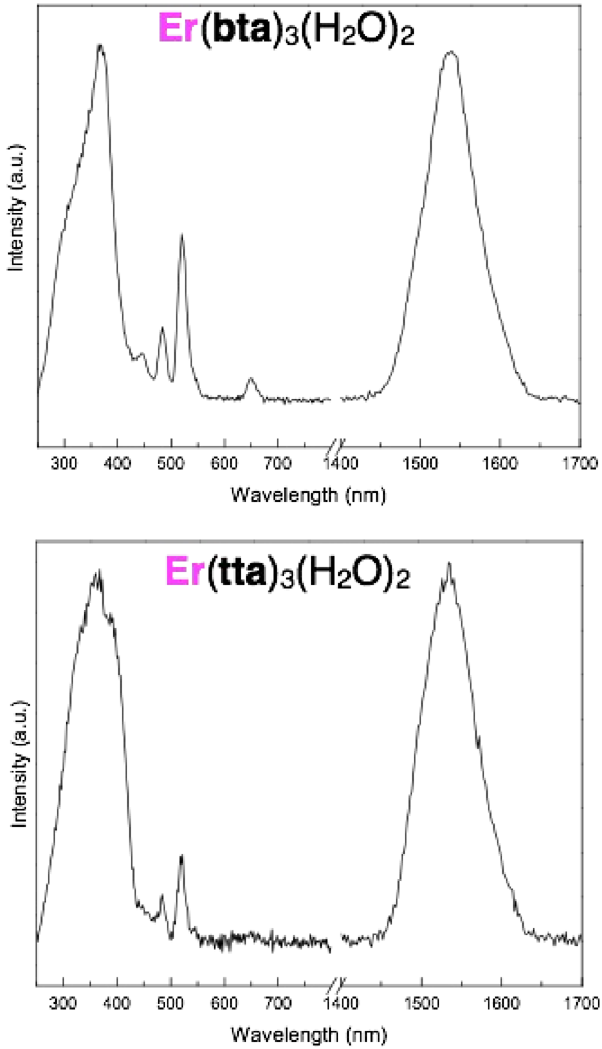


Fig. S4 Combined excitation-emission spectra of $Er^{3+}$ β-diketonate complexes (the spectra were recorded by exciting into the maximum of the broad excitation band and observing at the maximum of the strongest emission peak).

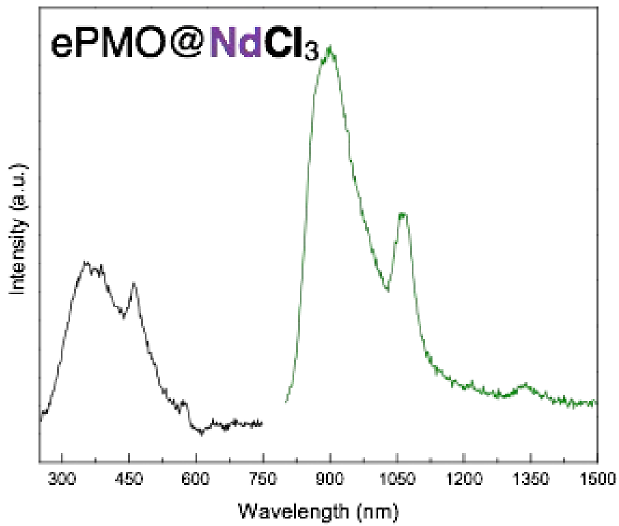


Fig. S5 Combined excitation-emission spectra of dppz-ePMO@$NdCl_3$ material (the spectra were recorded by exciting into the maximum of the broad excitation band and observing at the maximum of the strongest emission peak).

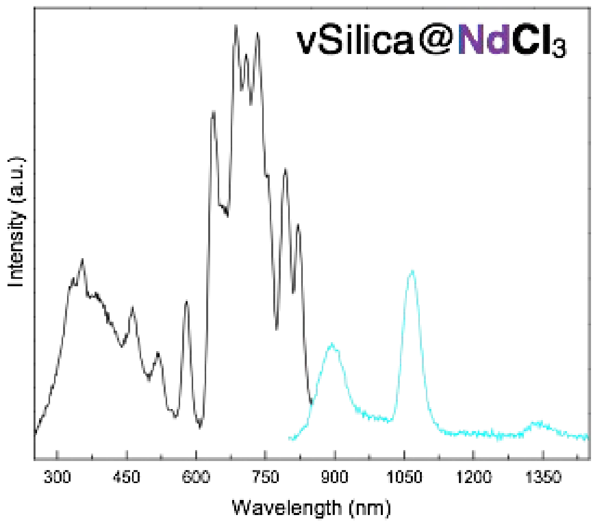


Fig. S6 Combined excitation-emission spectra of dppz-vSilica@$NdCl_3$ material (the spectra were recorded by exciting into the maximum of the broad excitation band and observing at the maximum of the strongest emission peak).

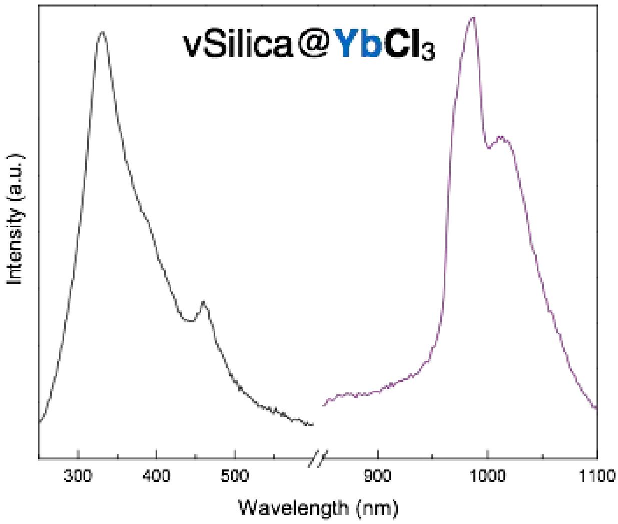


Fig. S7 Combined excitation-emission spectra of dppz-vSilica@$YbCl_3$ material (the spectra were recorded by exciting into the maximum of the broad excitation band and observing at the maximum of the strongest emission peak).*

*The signal of the ePMO@$YbCl_3$ material was too weak to record a sufficient excitation and emission spectrum. Also almost no signal was detected for the dppz-vSilica@$ErCl_3$ and dppz-ePMO@$ErCl_3$ materials, therefore they are not presented in the SI.

Table S1. Assignment of peaks observed in the excitation and emission spectra of dppz-ePMO@$LnL_3$ and dppz-vSilica@$LnL_3$ samples.

| dppz-ePMO@Nd(tta)$_3$ | | | |
|---|---|---|---|
| excitation | | emission | |
| wavelength [nm] | transition | wavelength [nm] | transition |
| 352.0 | π→π* | 898.0 | $^4F_{3/2} \rightarrow ^4I_{9/2}$ |
| 465.0 | $^4G_{11/2}$, $^2D_{3/2}$, $^2P_{3/2}$, $^2G_{9/2}$, $^2K_{15/2} \leftarrow ^4I_{9/2}$ | 1064.0 | $^4F_{3/2} \rightarrow ^4I_{11/2}$ |
| 517.0 | $^4G_{9/2}$, $^4G_{7/2}$, $^3K_{13/2} \leftarrow ^4I_{9/2}$ | 1335.0 | $^4F_{3/2} \rightarrow ^4I_{13/2}$ |
| 578.0 | $^2G_{7/2}$, $^4G_{5/2} \leftarrow ^4I_{9/2}$ | | |
| 685.0 | $^4F_{9/2} \leftarrow ^4I_{9/2}$ | | |
| 740.0 | $^4S_{3/2}$, $^4F_{7/2} \leftarrow ^4I_{9/2}$ | | |
| dppz-ePMO@Nd(bta)$_3$ | | | |
| excitation | | emission | |
| wavelength [nm] | transition | wavelength [nm] | transition |
| 327.0 | π→π* | 895.0 | $^4F_{3/2} \rightarrow ^4I_{9/2}$ |
| 461.0 | $^4G_{11/2}$, $^2D_{3/2}$, $^2P_{3/2}$, $^2G_{9/2}$, $^2K_{15/2} \leftarrow ^4I_{9/2}$ | 1064.0 | $^4F_{3/2} \rightarrow ^4I_{11/2}$ |
| 517.0 | $^4G_{9/2}$, $^4G_{7/2}$, $^3K_{13/2} \leftarrow ^4I_{9/2}$ | 1336.0 | $^4F_{3/2} \rightarrow ^4I_{13/2}$ |
| 576.0 | $^2G_{7/2}$, $^4G_{5/2} \leftarrow ^4I_{9/2}$ | | |
| 689.0 | $^4F_{9/2} \leftarrow ^4I_{9/2}$ | | |
| 738.0 | $^4S_{3/2}$, $^4F_{7/2} \leftarrow ^4I_{9/2}$ | | |
| dppz-vSilica@Nd(tta)$_3$ | | | |
| excitation | | emission | |
| wavelength [nm] | transition | wavelength [nm] | transition |
| 350.0 | π→π* | 899.0 | $^4F_{3/2} \rightarrow ^4I_{9/2}$ |
| 462.0 | $^4G_{11/2}$, $^2D_{3/2}$, $^2P_{3/2}$, $^2G_{9/2}$, $^2K_{15/2} \leftarrow ^4I_{9/2}$ | 1065.0 | $^4F_{3/2} \rightarrow ^4I_{11/2}$ |
| 521.0 | $^4G_{9/2}$, $^4G_{7/2}$, $^3K_{13/2} \leftarrow ^4I_{9/2}$ | 1335.0 | $^4F_{3/2} \rightarrow ^4I_{13/2}$ |
| 579.0 | $^2G_{7/2}$, $^4G_{5/2} \leftarrow ^4I_{9/2}$ | | |
| 680.0 | $^4F_{9/2} \leftarrow ^4I_{9/2}$ | | |
| 739.0 | $^4S_{3/2}$, $^4F_{7/2} \leftarrow ^4I_{9/2}$ | | |
| dppz-vSilica@Nd(bta)$_3$ | | | |
| excitation | | emission | |
| wavelength [nm] | transition | wavelength [nm] | transition |
| 336.0 | π→π* | 898.0 | $^4F_{3/2} \rightarrow ^4I_{9/2}$ |
| 461.0 | $^4G_{11/2}$, $^2D_{3/2}$, $^2P_{3/2}$, $^2G_{9/2}$, $^2K_{15/2} \leftarrow ^4I_{9/2}$ | 1069.0 | $^4F_{3/2} \rightarrow ^4I_{11/2}$ |
| 515.0 | $^4G_{9/2}$, $^4G_{7/2}$, $^3K_{13/2} \leftarrow ^4I_{9/2}$ | 1335.0 | $^4F_{3/2} \rightarrow ^4I_{13/2}$ |
| 576.0 | $^2G_{7/2}$, $^4G_{5/2} \leftarrow ^4I_{9/2}$ | | |
| 740.0 | $^4S_{3/2}$, $^4F_{7/2} \leftarrow ^4I_{9/2}$ | | |

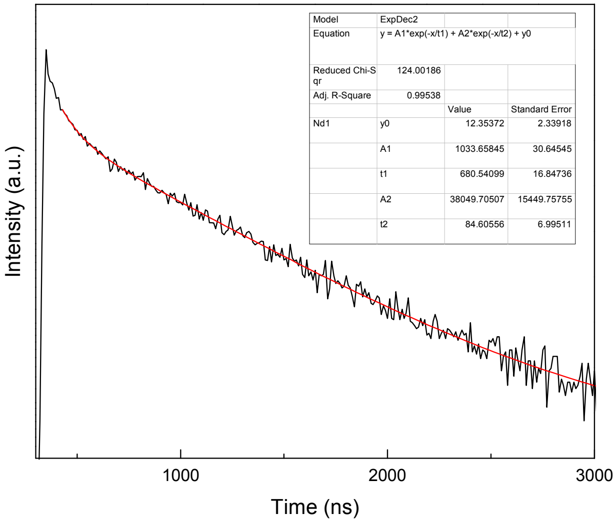


Fig. S8 Decay profile of dppz-ePMO@Nd(tta)$_3$.

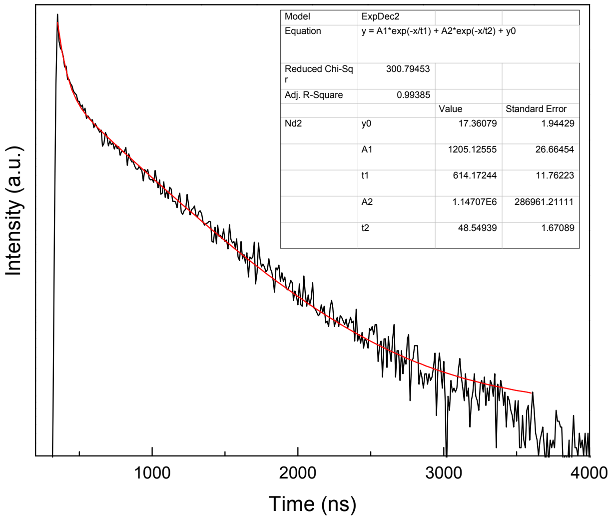


Fig. S9 Decay profile of dppz-ePMO@Nd(bta)$_3$.

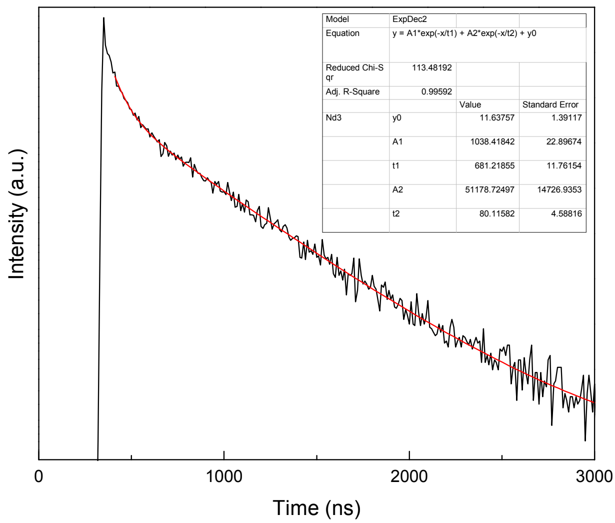


Fig. S10 Decay profile of dppz-vSilica@Nd(tta)$_3$.

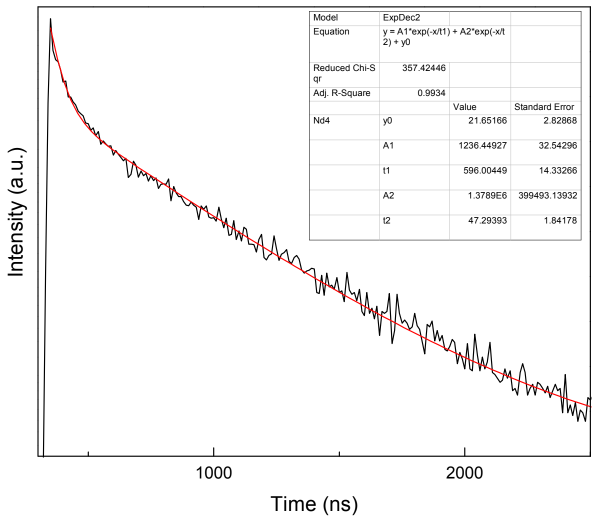


Fig. S11 Decay profile of dppz-vSilica@Nd(bta)$_3$.

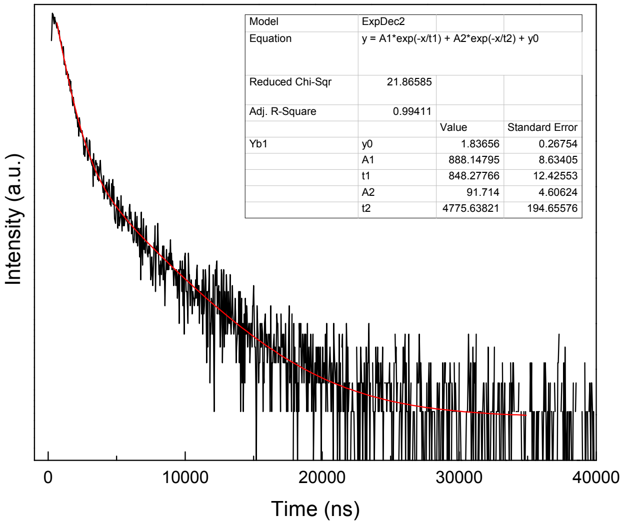


Fig. S12 Decay profile of dppz-ePMO@Yb(tta)$_3$.

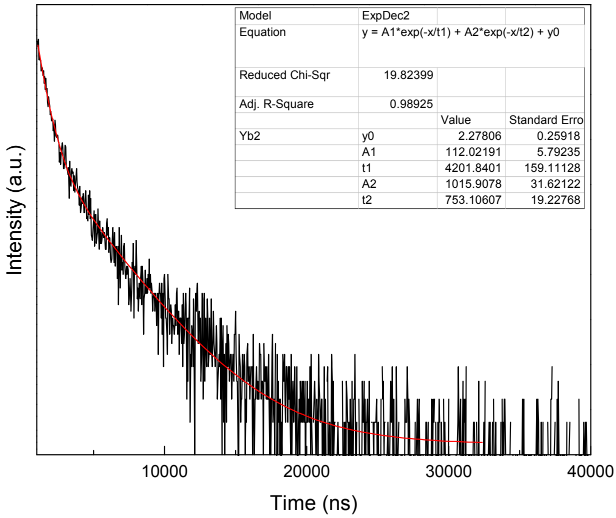


Fig. S13 Decay profile of dppz-ePMO@Yb(bta)$_3$.

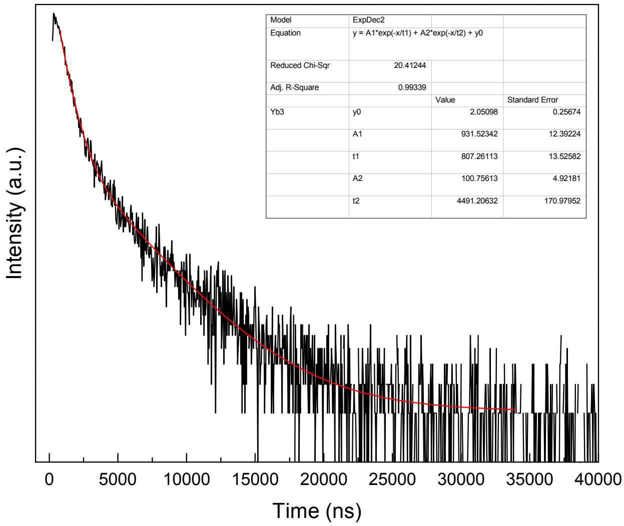


Fig. S14 Decay profile of dppz-vSilica@Yb(tta)$_3$.

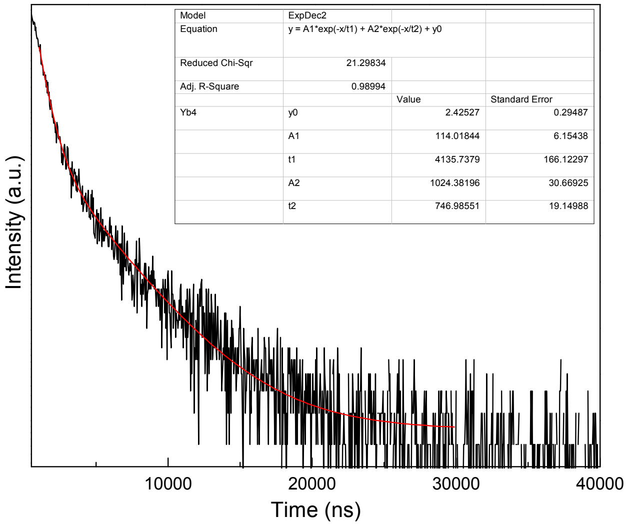


Fig. S15 Decay profile of dppz-vSilica@Yb(bta)$_3$.

$$\tau_{av} = \frac{A_1\tau_f^2 + A_2\tau_s^2}{A_1\tau_f + A_2\tau_s} \qquad (S1)$$

where $\tau_f$ is the fast decay time and $\tau_s$ is the slow decay time.

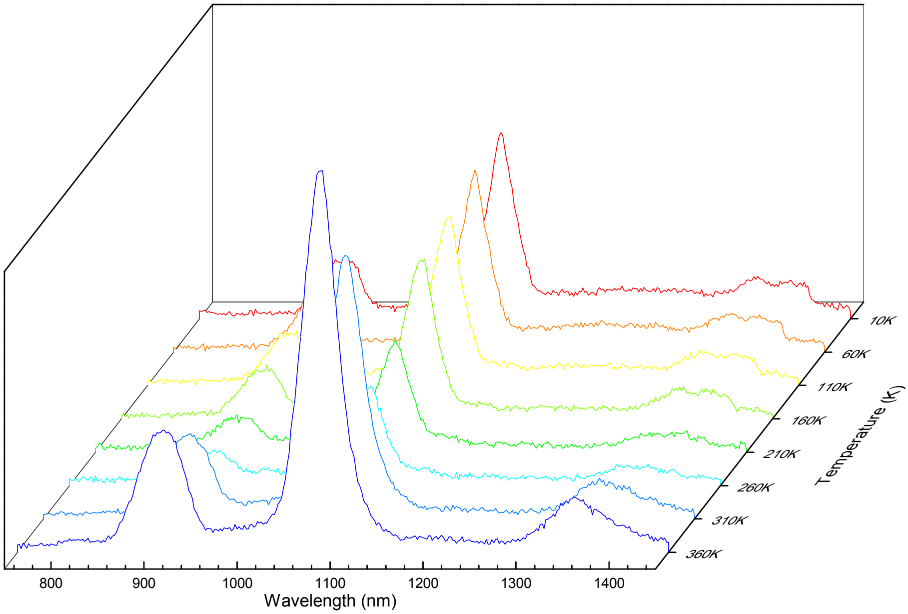


Fig. S16 Temperature dependent luminescence of $Nd(tta)_3 \cdot 2H_2O$ recorded in the 10 – 360 K temperature range.